

Q-switched Erbium-doped Fiber Laser Utilising a Saturable Absorber Based on Brass Nanoparticles

Ganesan Krishnan^{1,2*}, Siti Qistina Arora Talib^{1,2}, Afiq Arif Aminuddin Jafry³, Sulaiman Wadi Harun⁴, Muhammad Safwan Abd Aziz^{1,2}, Mundzir Abdullah⁵

¹Laser Center, Ibnu Sina Institute for Scientific and Industrial Research, Universiti Teknologi Malaysia, Johor Bahru, Malaysia

²Department of Physics, Faculty of Science, Universiti Teknologi Malaysia, 81310 Skudai, Johor, Malaysia

³School of Physics, Universiti Sains Malaysia, 11800 USM, Penang, Malaysia

⁴Department of Electrical Engineering, Faculty of Engineering, University of Malaya, 50603 Kuala Lumpur, Malaysia

⁵Institute of Nano Optoelectronics Research and Technology, Universiti Sains Malaysia, USM, 11800, Penang, Malaysia

*Email: k.ganesan@utm.my

Abstract

A passively Q-switched erbium-doped fiber laser was successfully demonstrated using brass nanoparticles embedded in Polyvinyl alcohol film as a saturable absorber. The brass nanoparticles were produced by ablating brass target in polyvinyl alcohol solution using Nd:YAG laser. The saturable absorber was characterised in terms of its morphology, elemental contents and optical properties. It was incorporated into a ring cavity to function as a Q-switcher for generating pulses. As the pump power was varied from 21 mW to 67 mW, the repetition rate increased from 38.74 kHz to 73.75 kHz while the corresponding output pulse width and pulse energy varied from 5.11 μ s to 2.473 μ s and 69.6 nJ to 145.6 nJ respectively. The output power characterised by the slope efficiency of 17.72 % and 10.74 mW of output power recorded at 67 mW pump power.

Keywords

pulsed laser, Q-switcher, saturable absorber

Introduction

Q-switched fiber lasers are widely researched due to their applications in optical communications, spectroscopy, industrial processing, sensing and medicine (Wen et al., 2021; Shakaty et al., 2022; Shangguan et al., 2023). The main advantages of Q-switched fiber lasers over Q-switched solid-state laser systems are their compactness and ease of maintenance. The saturable absorber (SA) is the critical component in a Q-switched laser cavity. Through the inclusion of SA

Submission: 2 August 2024; **Acceptance:** 2 September 2024



Copyright: © 2024. All the authors listed in this paper. The distribution, reproduction, and any other usage of the content of this paper is permitted, with credit given to all the author(s) and copyright owner(s) in accordance to common academic practice. This article is an open access article distributed under the terms and conditions of the Creative Commons Attribution (CC BY) license, as stated in the website: <https://creativecommons.org/licenses/by/4.0/>

into the cavity, the cavity loss is periodically modulated, and short optical pulses are generated as the laser output.

In the past decades, various materials were demonstrated as SA in fiber laser systems. One of the first materials that were studied for the SA application was semiconductor saturable absorber (SESAM) (Paschotta et al., 1999). However, the SESAM requires cost-intensive and complicated fabrication processes. Carbon nanotubes (CNTs) SA were also successfully utilised in various fiber lasers such as erbium doped fiber laser (EDFL) (Lazdovskaia et al., 2023), ytterbium doped fiber laser (YDFL) (Qiu et al., 2023) and thulium doped fiber laser (TDFL) (Chu et al., 2023). The dependency of spectral response range on chirality and diameter of the CNTs limits their practical applications (Salam et al., 2019). Black phosphorus (BP) had shown good performances as SA (Li et al., 2016; Huang et al., 2017) but its hydrophilic nature adversely affects its stability (Island et al., 2015). Two-dimensional materials, including transition metal dichalcogenides (Ahmad et al., 2022) and topological insulators (TIs) (Wang et al., 2021), were used to produce Q-switched pulses, yet complex production steps and low damage threshold are the common issues with these materials.

Recently, there are increasing studies on metal nanoparticles utilised as SA due to their fast response time and large third-order susceptibility (Zhang et al., 2023). Silver nanoparticles deposited onto the surface of polyvinyl alcohol (PVA) film was used as a SA to produce Q-switch pulses from EDFL (Rosdin et al., 2018). The output pulses had a maximum energy of 34.7 nJ and the shortest pulse width of 8.16 μ s. Gold nanoparticles in the form of composite were also successfully utilised as the SA in an EDFL to generate Q-switched pulses (Jiang et al., 2012). The pulses had an average pulse width of 3.2 μ s and an average repetition rate of 24.2 kHz. Apart from the noble metals, copper nanoparticles (Cu-NPs) and zinc nanoparticles (Zn-NPs) were also studied for their potential as SA in EDFL systems (Zaca-Morán et al., 2017; Muhammad et al., 2017). High repetition rate of 43.3 kHz was observed with Zn-NPs SA with pump power of 57.7 mW while short pulse width of 4.28 μ s was obtained with Cu-NPs SA. The nonlinear optical effects, such as saturable absorption, of elemental metals can be improved by forming nanocomposite using different materials (Anthony et al., 2008). It was shown that the nonlinear absorption coefficient of Ag-Au bilayered nanoprisms increased significantly compared to pure Au nanoprisms (Cesca et al., 2015). Brass is an alloy that primarily consists of various proportions of Cu and Zn added with small quantity of additional elements for improved machinability. Brass nanoparticles (brass-NPs) or nanoalloy were produced using laser ablation in liquid method with their physical and optical properties were characterised (Sukhov et al., 2014; Kazakevich et al., 2004). Brass-NPs are highly promising materials for antimicrobial, biomedical, and agrochemical applications (Antonoglou et al., 2019). The non-linear index and non-linear absorption coefficient of brass-NPs were determined using the Z-scan technique and the results showed a promising saturable absorption characteristic, as the measured nonlinear absorption coefficient was -3.4×10^{-4} cm/W (Abdullah et al., 2019).

This study explored the potential of brass nanoparticles (brass-NPs) SA in fiber laser systems. In this work, the brass-NPs embedded in polyvinyl alcohol (PVA) film was utilised as the SA in an EDFL system to generate the Q-switched laser pulses. The physical, chemical and optical characteristics of the saturable absorber were analysed. Additionally, the performance characteristics of Q-switched laser were also evaluated. The Q-switched laser output was successfully generated with peak power of 58.9 mW and pulse width of 2.47 μ s with a pump power of 67 mW.

Methodology

Figure 1 illustrates the setup of pulsed laser ablation in liquid system that was used to produce the brass-NPs. A Q-switched Nd:YAG laser with 8 ns pulse duration and an output wavelength of 1064 nm was utilised to ablate a brass plate immersed in a PVA solution. The repetition rate of laser pulses was 10 Hz and the laser energy per pulse was 290 mJ. The PVA solution was prepared by mixing 0.2 g of PVA powder with 20 ml of distilled water. The mixture was stirred and heated within 50 – 60 °C for 3 hours. During the laser ablation process, laser pulses were focused through 100 mm focusing lens onto the brass target in PVA solution. The duration of ablation process was 640 seconds, where a total of 6400 laser shots were deposited on the target during this period. The cuvette with the PVA solution and brass target was rotated with a stepper motor during the laser ablation to make the solution homogenous and to avoid formation of the craters on the surface of the target. At the end of laser ablation process, brass-NPs in the PVA solution were obtained. The transmission electron microscope (TEM) and Energy Dispersive X-Ray (EDX) analyses were done on the brass-NPs in PVA solution. The remaining solution was poured onto a stainless-steel plate and left to dry for 3 days, resulting in a PVA thin film with brass-NPs embedded. The wavelength operation of the thin film SA was examined. A white light source (YOKOGAWA, ANDO AQ-4303B) was launched onto the SA via an FC/PC fiber-ferrule. The light transmitted through the SA was then collected by an optical spectrum analyser (ANRITSU, MS9710C) with a wavelength span of 1050 to 1650 nm that was connected to another fiber-ferrule on the other side of the SA.

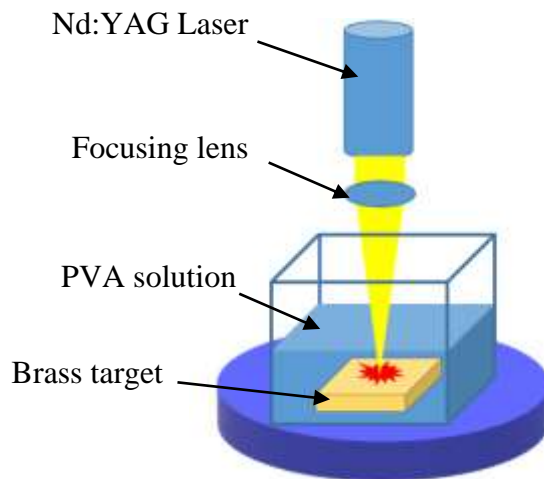


Figure 1. Laser ablation setup for brass-NPs production

Figure 2 depicts the Q-switched EDFL setup with brass-NPs SA. The pumping source for the laser system was a 980 nm laser diode. The laser diode output beam was coupled to a 13.4 m long EDFL ring cavity via a 980/1550 nm wavelength division multiplexer (WDM). The main components in the ring cavity were an erbium-doped fiber (EDF), an isolator, a brass-NPs SA and an optical coupler. The EDF with a length of 2.4 m functions as the gain medium with absorption cross section of 23 dB/m at 980 nm. The core of EDF had a diameter of 5.8 μm and numerical

aperture of 0.24. The isolator limited the light to propagate in a single direction in the ring cavity. The brass-NPs SA with an area of approximately 1mm^2 was placed in between two fiber ferrules in the fiber adaptor. Index matching gel was applied between the fiber ferrules and the SA to reduce parasitic reflections. 20% of the intracavity light was coupled out from the cavity with the optical coupler with 80:20 coupling ratio for the laser output measurements. The Q-switched laser outputs at various pump powers were characterised by its output power, output wavelength characteristics and temporal properties. The output power measurement was done with a Thorlabs PM100USB power meter while a YOKOGAWA AQ6370D optical spectrum analyser (OSA) was utilised to record the laser output wavelength spectrum. An InGaAS photodetector connected to GWINSTEK GDS-3352 digital oscilloscope and 7.8 GHz RF ANRITSU MS2683A spectrum analyser was employed to detect the temporal characteristics of the Q-switched pulses, which were the pulse width and repetition rate. The peak output powers and pulse energies at various pump powers were calculated based on the recorded output powers, pulse widths and repetition rates.

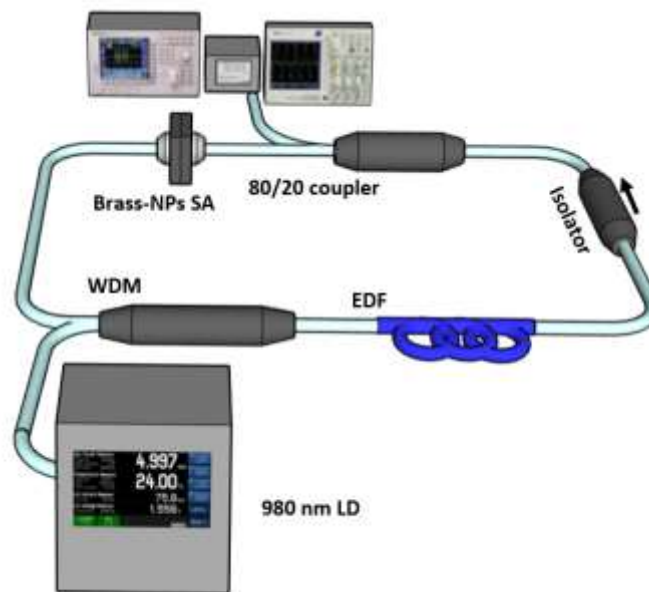


Figure 2. Q-switched EDFL laser setup with brass-NPs SA.

Results and Discussion

Figure 3 shows the results of the TEM and EDX analyses of the brass-NPs in PVA solution. Based on TEM micrograph in Fig. 3 (a), the morphology of brass-NPs is sphere with core-shell structure. This result agrees with previous works where brass-NPs were produced with laser ablation in liquid method (Sukhov et al., 2014; Kazakevich et al., 2004). The diameter of the brass NPs ranges from 18.9 nm to 41.8 nm, as seen in Fig. 3 (a). The EDX point analysis verified the presence of carbon (C), oxygen (O), copper (Cu) and zinc (Zn). The presence of brass-NPs in the sample was verified due to the detection of Cu and Zn, which are the main elemental constituents of the brass plate. The detection of the C and O in the EDX analysis are due to the presence of PVA polymer in the sample. As for the linear absorption characteristics of the brass-NPs SA, about 1.5 dB of absorption is detected at the operation wavelength of EDFL at 1560 nm as shown in Figure 4.

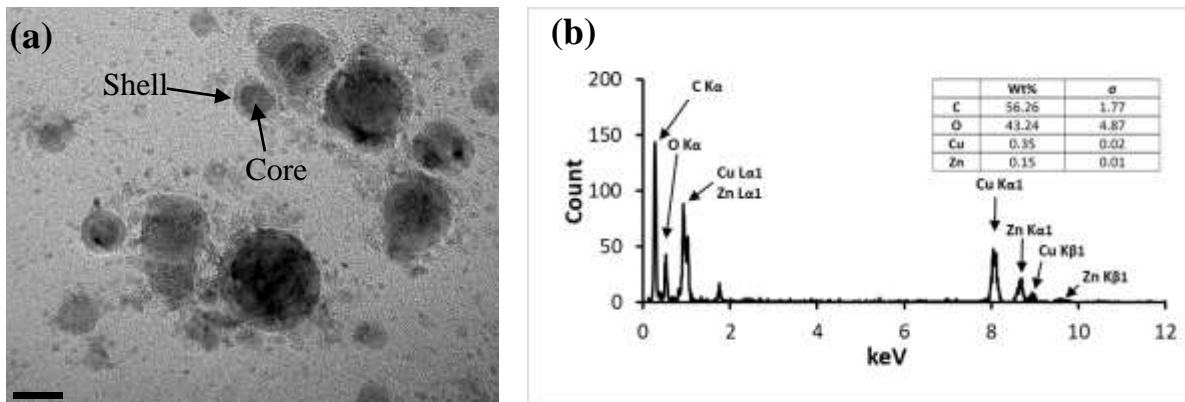


Figure 3. Brass NPs characterisations: (a) TEM analysis and (b) EDX analysis.

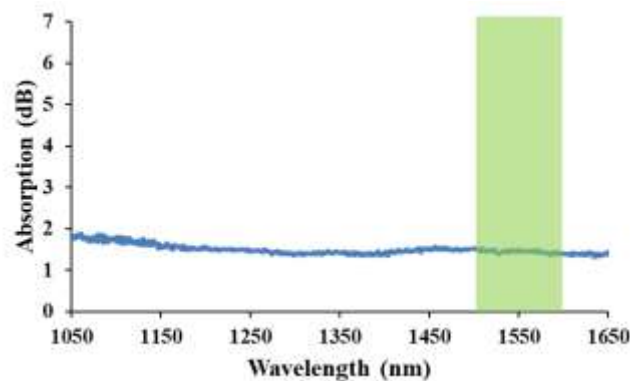


Figure 4. Absorption curve of the brass-NPs SA

The EDFL cavity started to operate in continuous wave regime at a low pump power of 16 mW, indicating the splice losses between optical components were small. As the pump power was raised towards 21 mW, a stable Q-switching operation was visible on the oscilloscope. A steady Q-switched pulse was maintained up to 67 mW of pump power. However, the pulse started to mitigate and become unstable as the pump power was raised from 71 to 90 mW. The Q-switched operation eventually disappeared as the pump power adjusted above 90 mW. The stability of the generated Q-switched was superior as stable pulses were obtained when the pump power was adjusted within 21 to 67 mW. Figure 5 (a) depicts the optical spectrum of Q-switched (blue line) and continuous wave (orange line) at the pump power of 67 mW, which was the maximum achievable pump power for the stable Q-switching operation. The incorporation of brass-NPs into the laser cavity causes the center wavelength to shift from 1564 to 1560 nm. The SA modulates cavity loss inside the EDFL, thus altering the operating wavelength of the laser to a shorter near-infrared spectrum. Temporal characteristics of the Q-switched EDFL were captured using an oscilloscope, as shown in Figure 5 (b). The oscilloscope trace recorded within 150 μ s duration shows a few uniform pulses without distinct amplitude modulation, indicating a low timing jitter inside the EDFL cavity (Qin et al., 2014). The enlarged graphic of two pulses envelope was also plotted to express the pulse width and pulses interval of generated Q-switched, which were 2.47 μ s and 13.56 μ s, respectively. The stability of generated pulses was further investigated using an RF spectrum analyser. Figure 5 (c) represents the spectrum captured within the 1500 kHz

frequency span at the pump power of 67 mW. An inset image showing a fundamental frequency of 73.75 kHz was also captured with a signal-to-noise ratio (SNR) of 70.86 dB. The graph shows many harmonics with multiple peaks that gradually decline, indicating a stable Q-switched laser operation. As shown earlier in Figure 5 (b), the oscilloscope trace owns an interval between two pulses of 13.56 μs which corresponds to the repetition rate of 73.75 kHz, agreeing well with the value recorded on the RF spectrum analyzer.

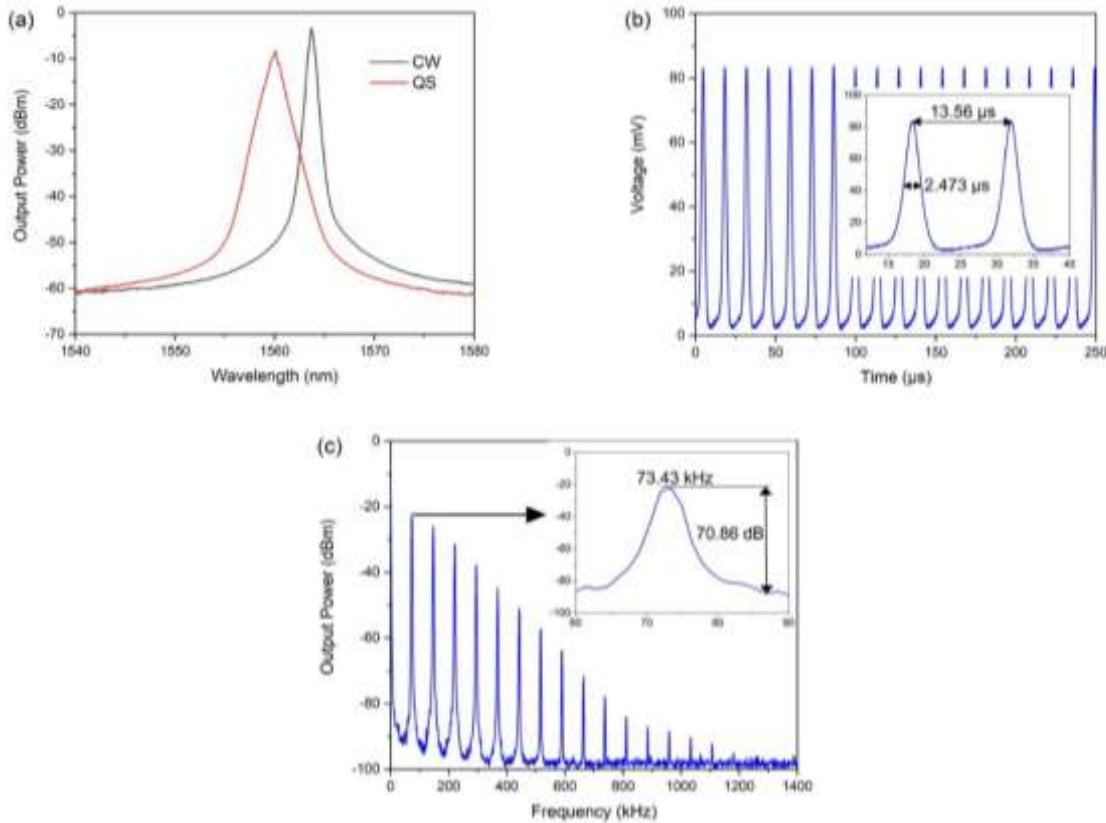


Figure 5. Spectral and temporal performances: (a) OSA spectrum of CW and QS, (b) oscilloscope trace, and (c) RF spectrum of QS at pump power of 67 mW.

Figure 6 (a) denotes the repetition rate and pulse width as the pump power tuned between 21 to 67 mW. A linearly increasing pattern of repetition rate against pump power is observed in the figure. The minimum repetition rate obtained was 38.74 kHz at the lowest pump power of 21 mW, whereas the maximum repetition rate was 73.75 kHz. In contrast, the pulse width declined from 5.11 to 2.47 μs as the pump power raised within the range stated earlier. The pulse width produced with brass-NPs SA in this work is shorter than that of silver nanoparticles SA, which was 8.16 μs (Rosdin et al., 2018). The signal was further analysed using an optical power meter to investigate the performance of Q-switched EDFL within an interval of pump power. The pump power was adjusted within 21 mW to 67 mW, which resulted in stable Q-switched pulses, as shown in Figure 6 (b). As indicated in the graph, data points in black color represent the graph of output power as a function of pump power. The output power escalates from 2.7 to 10.74 mW with the increment of pump power within the Q-switching pumping range. The linearly increasing line of

output power against pump power also reveals a high slope efficiency of 17.72 %, which was attributed to the optimum configuration and length of the EDFL cavity. The calculated pulse energy was also plotted in the same graph in Figure 6 (b) with a maximum value of 145.6 nJ at the pump power of 67 mW. Finally, the graph of peak power as a function of pump power was shown in Figure 6 (c). As the pump power was tuned from 21 to 67 mW, the peak power rose from 13.6 to 58.9 mW.

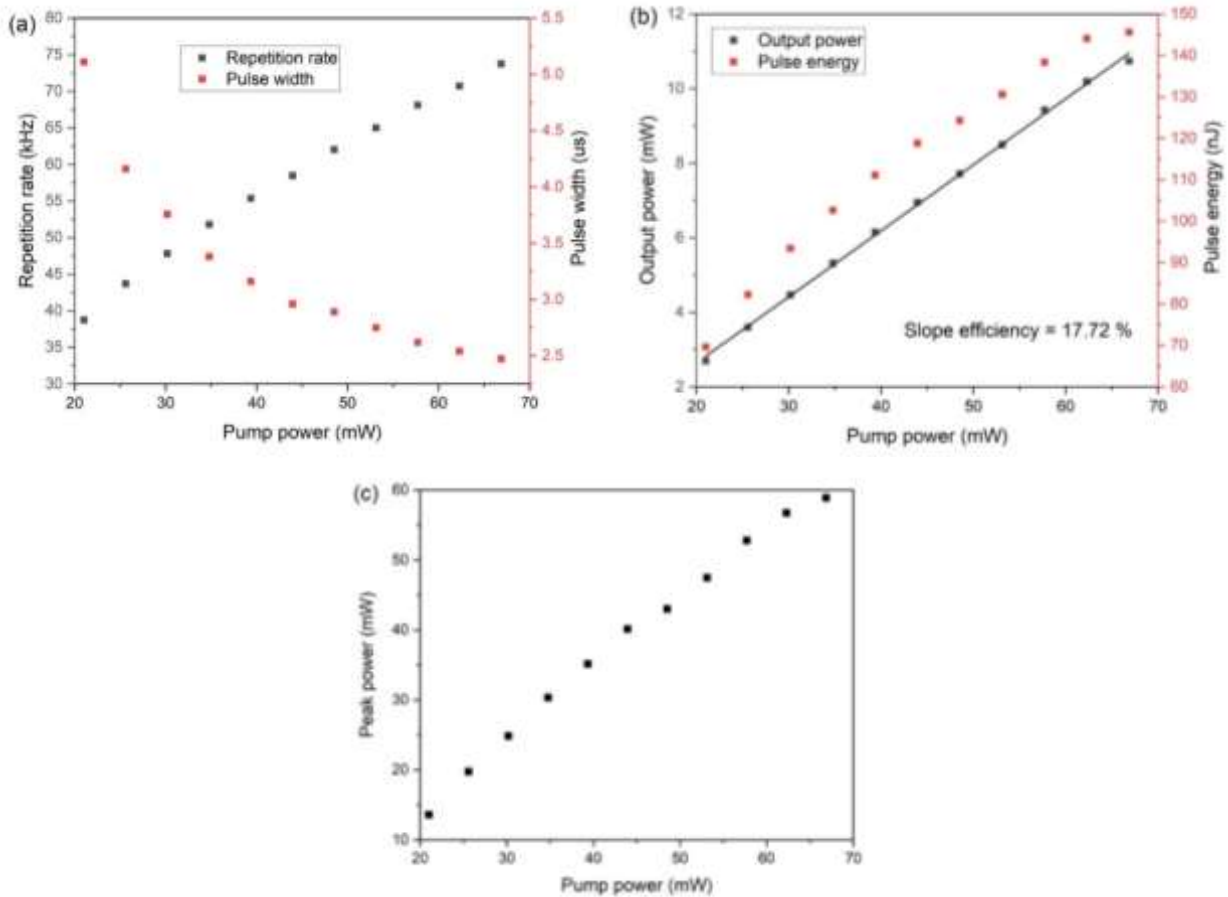


Figure 6. Q-switched EDFL laser performances: (a) repetition rate and pulse duration variation with pump power, (b) output power and pulse energy variation with pump power, and (c) peak power variation with pump power.

Conclusion

Stable Q-switched laser output from EDFL was successfully demonstrated by including brass-NPs thin film SA in ring cavity arrangement. The self-starting Q-switched pulses were obtained at and beyond the pump power of 21 mW. The highest repetition rate of 73.75 kHz and shortest pulse width of 2.473 μ s were recorded at 67 mW pump power in this study. The output power increased linearly with pump power where the slope efficiency was 17.72 %, and the highest output power recorded was 10.74 mW. The brass-NPs SA showed a promising performance in the EDFL system, and it can be implemented into other fiber lasers, such as YDFL, in future works.

Acknowledgements

This work was mainly supported by the Fundamental Research Grants Scheme (FRGS) with grant number FRGS/1/2024/STG07/UTM/02/8 - R.J130000.7854.5F704) from the Ministry of Higher Education (MOHE) Malaysia, and also supported by UTMER, grant number Q.J130000.3854.31J74, Universiti Teknologi Malaysia. The second author also wishes to thank the Ministry of Education Malaysia for providing MyBrainSc Scholarship for her postgraduate study.

References

- Abdullah, M., Bakhtiar, H., Aziz, M. S. A., Krishnan, G., Ropi, N. A. M., Kasim, N., & Adnan, N. N. (2019). Thermally induced optical nonlinearity in colloidal alloy nanoparticles synthesized by laser ablation. *Applied Physics B*, 125, 1-9. <https://link.springer.com/article/10.1007/s00340-019-7271-3>
- Ahmad, H., Kahar, N. H. A., Yusoff, N., Samion, M. Z., Reduan, S. A., Ismail, M. F., ... & Sahu, J. K. (2022). Passively Q-switched 1.3 μm bismuth doped-fiber laser based on transition metal dichalcogenides saturable absorbers. *Optical Fiber Technology*, 69, 102851. <https://doi.org/10.1016/j.yofte.2022.102851>
- Anthony, J. K., Kim, H. C., Lee, H. W., Mahapatra, S. K., Lee, H. M., Kim, C. K., ... & Rotermu, F. (2008). Particle size-dependent giant nonlinear absorption in nanostructured Ni-Ti alloys. *Optics express*, 16(15), 11193-11202. <https://doi.org/10.1364/OE.16.011193>
- Antonoglou, O., Founta, E., Karagkounis, V., Pavlidou, E., Litsardakis, G., Mourdikoudis, S., ... & Dendrinou-Samara, C. (2019). Structure differentiation of hydrophilic brass nanoparticles using a polyol toolbox. *Frontiers in Chemistry*, 7, 817. <https://doi.org/10.3389/fchem.2019.00817>
- Cesca, T., Michieli, N., Kalinic, B., Sánchez-Espinoza, A., Rattin, M., Russo, V., ... & Mattei, G. (2015). Nonlinear absorption tuning by composition control in bimetallic plasmonic nanoprisms arrays. *Nanoscale*, 7(29), 12411-12418. <https://doi.org/10.1039/C5NR01715G>
- Chu, S., Sun, D., Chen, J., Sun, L., Shi, W., Lu, J., ... & Ruan, S. (2023). Passively mode-locked thulium-doped fiber laser based on a SWCNTs@ AFI saturable absorber. *Infrared Physics & Technology*, 128, 104479. <https://doi.org/10.1016/j.infrared.2022.104479>
- Huang, K. X., Lu, B. L., Li, D., Qi, X. Y., Chen, H. W., Wang, N., ... & Bai, J. T. (2017). Black phosphorus flakes covered microfiber for Q-switched ytterbium-doped fiber laser. *Applied optics*, 56(23), 6427-6431. <https://doi.org/10.1364/AO.56.006427>
- Island, J. O., Steele, G. A., van der Zant, H. S., & Castellanos-Gomez, A. (2015). Environmental instability of few-layer black phosphorus. *2D Materials*, 2(1), 011002. <https://doi.org/10.1088/2053-1583/2/1/011002>
- Jiang, T., Xu, Y., Tian, Q., Liu, L., Kang, Z., Yang, R., ... & Qin, W. (2012). Passively Q-switching induced by gold nanocrystals. *Applied Physics Letters*, 101(15). <https://doi.org/10.1063/1.4759120>

- Kazakevich, P. V., Voronov, V. V., Simakin, A. V., & Shafeev, G. A. (2004). Production of copper and brass nanoparticles upon laser ablation in liquids. *Quantum Electronics*, 34(10), 951. <https://doi.org/10.1070/qe2004v034n10abeh002756>
- Lazdovskaia, U. S., Orekhov, I. O., Ismaeel, A., Feifei, Y., Dvoretzkiy, D. A., Sazonkin, S. G., ... & Davydov, V. A. (2023). High-Density Well-Aligned Single-Walled Carbon Nanotubes for Application as a Saturable Absorber with a High-Pass Filter Effect in an Erbium-Doped Ultra-Short-Pulse Fiber Laser. *ACS Applied Nano Materials*, 6(24), 23410-23417. <https://doi.org/10.1021/acsanm.3c04766>
- Li, D., Castillo, A. E. D. R., Jussila, H., Ye, G., Ren, Z., Bai, J., ... & Bonaccorso, F. (2016). Black phosphorus polycarbonate polymer composite for pulsed fibre lasers. *Applied Materials Today*, 4, 17-23. <https://doi.org/10.1016/j.apmt.2016.05.001>
- Muhammad, A. R., Ahmad, M. T., Zakaria, R., Rahim, H. R. A., Yusoff, S. F. A. Z., Hamdan, K. S., ... & Harun, S. W. (2017). Q-switching pulse operation in 1.5- μm region using copper nanoparticles as saturable absorber. *Chinese physics letters*, 34(3), 034205. <https://doi.org/10.1088/0256-307x/34/3/034205>
- Paschotta, R., Häring, R., Gini, E., Melchior, H., Keller, U., Offerhaus, H. L., & Richardson, D. J. (1999). Passively Q-switched 0.1-mJ fiber laser system at 1.53 μm . *Optics letters*, 24(6), 388-390. <https://doi.org/10.1364/OL.24.000388>
- Qin, P., Song, Y., Kim, H., Shin, J., Kwon, D., Hu, M., ... & Kim, J. (2014). Reduction of timing jitter and intensity noise in normal-dispersion passively mode-locked fiber lasers by narrow band-pass filtering. *Optics express*, 22(23), 28276-28283. <https://doi.org/10.1364/oe.22.028276>
- Qiu, H., Sun, M., Yao, Y., Pan, Y., Wang, X., & Wang, J. (2023). Passively mode-locked Yb-doped fiber laser based on CNT-film sandwiched between the multimode fiber connectors. *Optik*, 281, 170791. <https://doi.org/10.1016/j.ijleo.2023.170791>
- Rosdin, R. Z. R., Ahmad, M. T., Jusoh, Z., Arof, H., & Harun, S. W. (2018). All-fiber Q-switched fiber laser based on silver nanoparticles saturable absorber. *Digest Journal of Nanomaterials and Biostructures*, 13, 1159-1164. URL: https://chalcogen.ro/1159_RosdinRZR.pdf
- Salam, S., Al-Masoodi, A. H. H., Al-Hiti, A. S., Al-Masoodi, A. H., Wang, P., Wong, W. R., & Harun, S. W. (2019). FIRpic thin film as saturable absorber for passively Q-switched and mode-locked erbium-doped fiber laser. *Optical fiber technology*, 50, 256-262. <https://doi.org/10.1016/j.yofte.2019.04.005>
- Shakaty, A. A., Hmood, J. K., Mahdi, B. R., Mahdi, R. I., & Al-Azzawi, A. A. (2022). Q-switched erbium-doped fiber laser based on nanodiamond saturable absorber. *Optics & Laser Technology*, 146, 107569. <https://doi.org/10.1016/j.optlastec.2021.107569>
- Shangguan, M., Yang, Z., Shangguan, M., Lin, Z., Liao, Z., Guo, Y., & Liu, C. (2023). Remote sensing oil in water with an all-fiber underwater single-photon Raman lidar. *Applied Optics*, 62(19), 5301-5305. <https://doi.org/10.1364/ao.488872>
- Sukhov, I. A., Shafeev, G. A., Voronov, V. V., Sygletou, M., Stratakis, E., & Fotakis, C. (2014). Generation of nanoparticles of bronze and brass by laser ablation in liquid. *Applied Surface Science*, 302, 79-82. <https://doi.org/10.1016/j.apsusc.2013.12.018>
- Wang, T., Yu, Q., Guo, K., Shi, X., Kan, X., Xu, Y., ... & Zhou, P. (2021). Sb₂Te₃ topological insulator for 52 nm wideband tunable Yb-doped passively Q-switched fiber laser. *Frontiers of Information Technology & Electronic Engineering*, 22(3), 287-295. <https://doi.org/10.1631/fitee.2000577>

- Wen, Z., Wang, K., Chen, S., Chen, H., Qi, X., Lu, B., & Bai, J. (2021). Narrow bandwidth Q-switched Erbium-doped fiber laser based on dynamic saturable absorption filtering effect. *Optics & Laser Technology*, 140, 107045. <https://doi.org/10.1016/j.optlastec.2021.107045>
- Zaca-Morán, P., Ortega-Mendoza, J. G., Lozano-Perera, G. J., Gómez-Pavón, L. C., Pérez-Sánchez, G. F., Padilla-Martínez, J. P., & Felipe, C. (2017). Passively Q-switched erbium-doped fiber laser based on Zn nanoparticles as a saturable absorber. *Laser Physics*, 27(10), 105101. <https://doi.org/10.1088/1555-6611/aa83e0>
- Zhang, Y., Wen, S., Su, X., Wang, Y., Li, G., Xie, Y., ... & Zhang, B. (2023). Sub-100 fs Yb: CALGO laser based on gold nanoparticles saturable absorber. *Optik*, 288, 171169. <https://doi.org/10.1016/j.ijleo.2023.171169>